# SUPPLEMENTARY INFORMATION

## Mechanical and Morphological Bond Line Properties of Silver Birch Wood Pretreated by Aqueous Extraction

**Journal:** Journal of Wood Chemistry and Technology (Taylor and Francis)

**Authors:**

Max ENGELHARDT[1,*]
orcid.org/0000-0002-9781-7476 (engelhardt@hfm.tum.de)

Thomas BÖGER[1]
orcid.org/0000-0001-8747-8506 (boeger@hfm.tum.de)

Michael GIGL[2]
orcid.org/0000-0002-5617-9236 (michael.gigl@tum.de)

Chen MENG[2]
orcid.org/0000-0002-5968-6719 (chen.meng@tum.de)

Klaus RICHTER[1]
orcid.org/0000-0002-6583-0254 (richter@hfm.tum.de)

Antoni SANCHEZ-FERRER[1,*]
orcid.org/0000-0002-1041-0324 (sanchez@hfm.tum.de)

[1] Chair of Wood Science, TUM School of Life Sciences, Technical University of Munich

[2] Bavarian Center for Biomolecular Mass Spectrometry, TUM School of Life Sciences, Technical University Munich

## Figures



## Tables

## Extraction Analysis

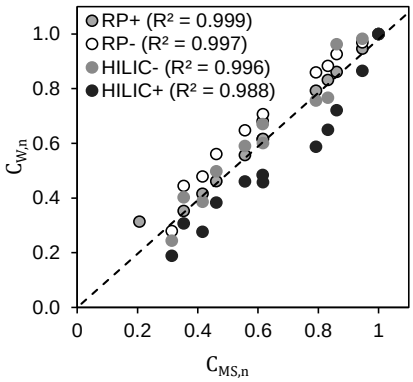


Figure SI–1 Comparison of normalized cumulative sums of extractives content by weight ($C_{W,n}$) and normalized cumulative sum of sample-weight-adjusted and $m/z$ weighted MS peak areas ($C_{MS,n}$). The dashed line indicates the linear regression on data of all modes, the $R^2$ values correspond to the regressions of individual UHPLC measurement modes.

A comparison of the relative detected abundance and observed LC separation mechanism for all four UHPLC/MS modes of measurement are shown in Table SI–1.

Table SI–1: Compound classes detected by UHPLC/MS modes – comparison of detected abundance and separation mechanisms. SX (size exclusion – negative correlation), AF (affinity - positive correlation) and UD (undetermined - low correlation) are the possible separation mechanisms (m/z~$t_r$ correlation). The symbols + / o / - correspond to the highest / intermediate / low ionization/detected abundance.

| **compound class** | **UHPLC/MS detection mode** | | | |
|---|---|---|---|---|
| | HILIC- | HILIC+ | RP- | RP+ |
| fatty acids | o SX | o UD | + AF | - AF |
| glycerolipids | - UD | + AF | o UD | n. d. |
| phenols | o UD | - UD | - UD | + UD |
| phenolic glycosides | o UD | - UD | + UD | - AF |
| phospholipids | o UD | + AF | - UD | - UD |
| polyphenols | n. d. | o UD | + UD | - UD |
| saccharides | n. d. | n. d. | + SX | o SX |
| unknowns | o UD | + UD | - UD | o UD |

An overview of UHPLC/MS results for all modes regarding $m/z$, retention time and $\langle\tau\rangle$, see Figure SI–2 to Figure SI–4 below.

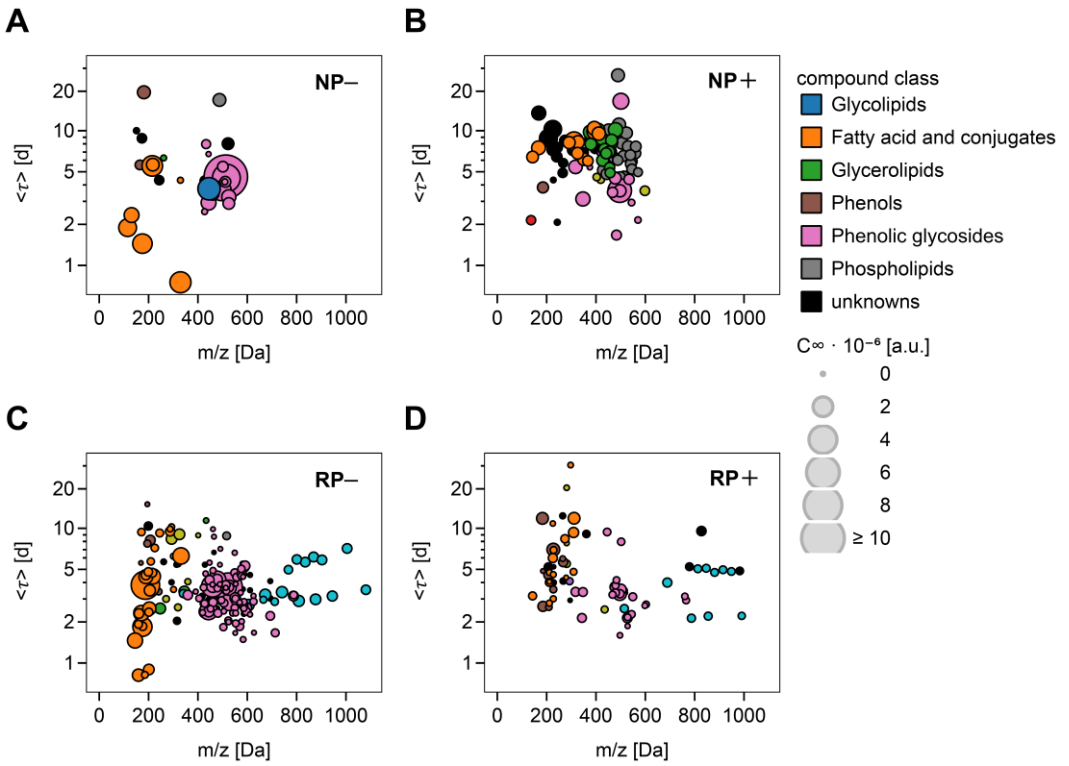


Figure SI–2: UHPLC-ESI-TOF-MS extractives analysis results – Average lifetime $\langle\tau\rangle$ as a function of $m/z$ (A: HILIC column and negative electrospray ionization; B: HILIC column and positive electrospray ionization; C: Reverse phase column and negative electrospray ionization; D: Reverse phase column and positive electrospray ionization.)

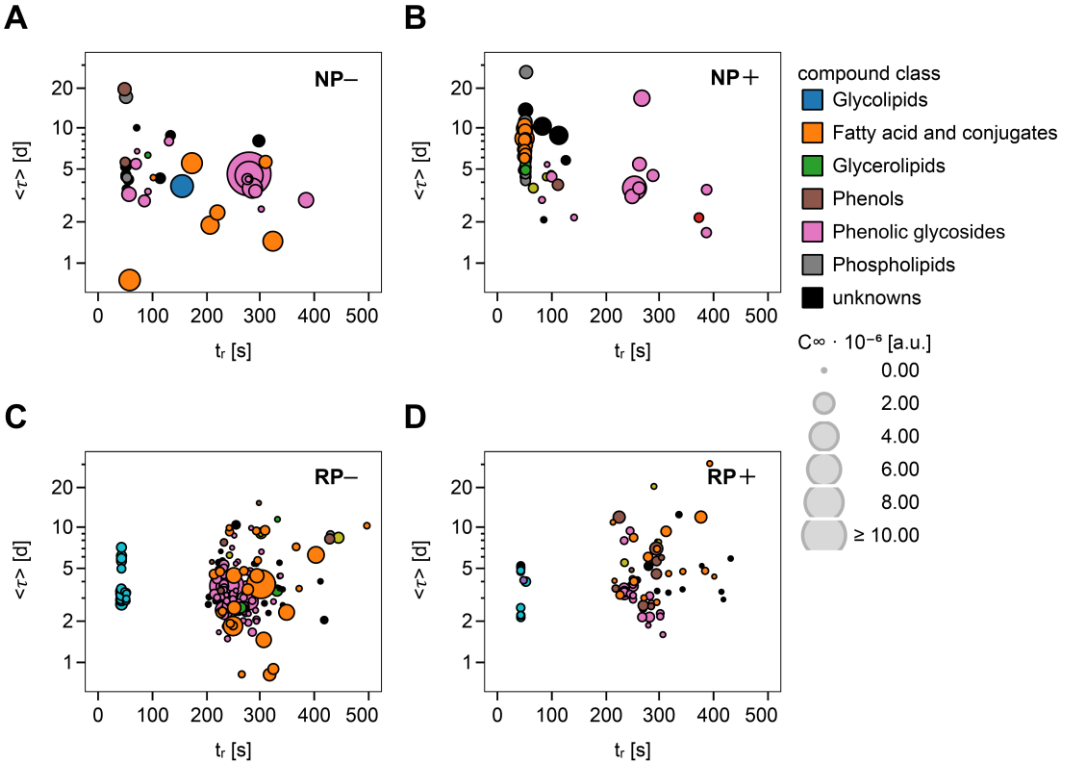


Figure SI–3: UHPLC-ESI-TOF-MS extractives analysis results – Average lifetime $\langle\tau\rangle$ as a function of retention time $t_r$ (A: HILIC column and negative electrospray ionization; B: HILIC column and positive electrospray ionization; C: Reverse phase column and negative electrospray ionization; D: Reverse phase column and positive electrospray ionization.)

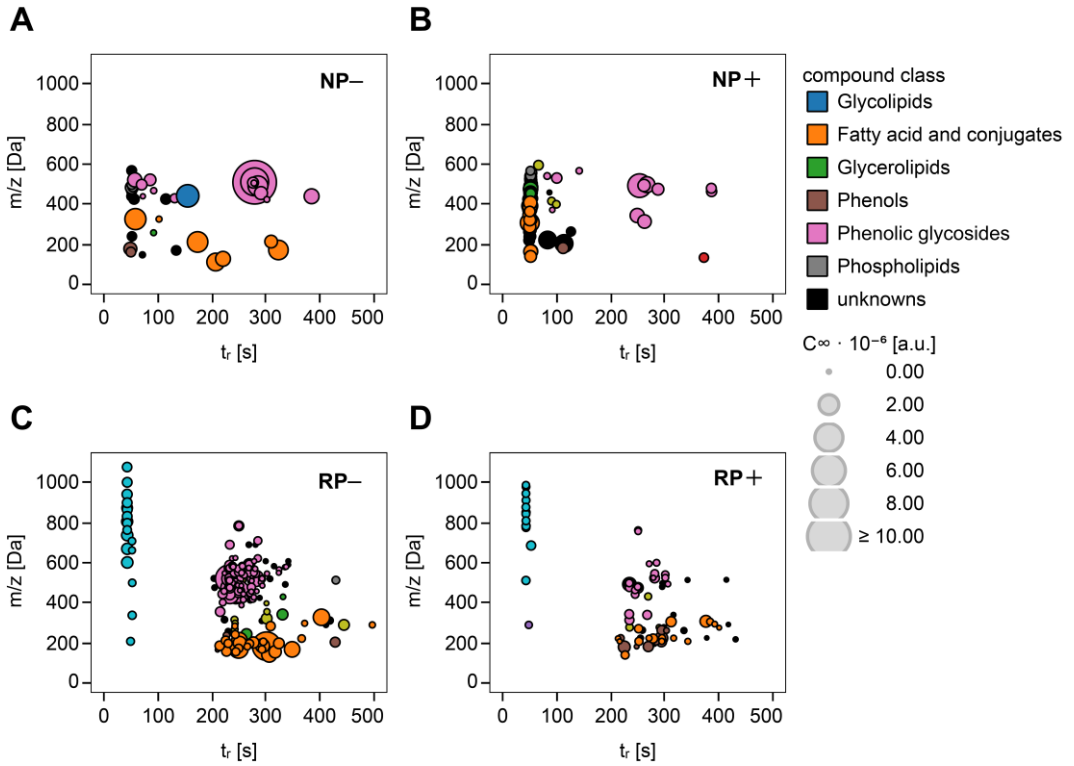


Figure SI–4: UHPLC-ESI-TOF-MS extractives analysis results – $m/z$ as a function of retention time $t_r$ (A: HILIC column and negative electrospray ionization; B: HILIC column and positive electrospray ionization; C: Reverse phase column and negative electrospray ionization; D: Reverse phase column and positive electrospray ionization.)

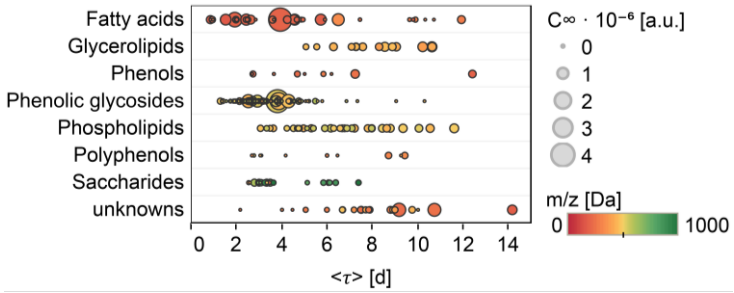


Figure SI–5: Equivalent lifetime <τ> values (Eq. 4) of the extracted compounds by class (shown for modes with the highest detection rate). The mass-to-charge ratio ($m/z$) is indicated by color, and the equilibrium estimate of adjusted abundance $C_\infty$ is indicated by the dot size.

In Figure SI–6B, a comparison of the MS abundance data to the gravimetric results of the relative extractives concentration per weight, *i.e.*, extraction degree $ED$, reveals some deviations in the release pattern compared to MS data. This deviation can be due to both methodological factors regarding, *e.g.*, the electrospray ionization, variations in the detector's response factor, uncertainty in equilibrium estimations via the exponential fittings, possible bias from compound review procedures of MS data, and the presence of substances undetectable for the MS setup outside of the $m/z$-range, such as inorganic compounds. The amount of inorganics in the

extractives was estimated by the ash content (furnace method, 60 min at 550 °C) to be 11% (W/W), corresponding to a mineral content of 0.13% (W/W) in the wood.

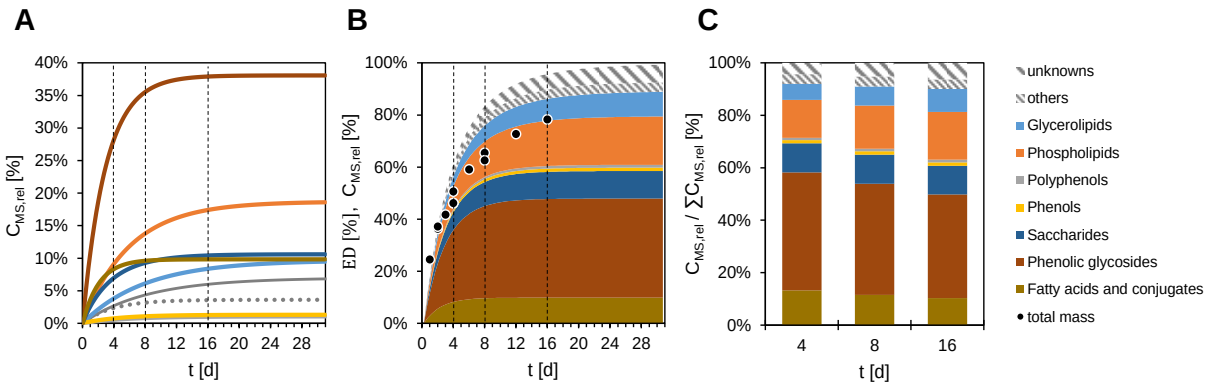


Figure SI–6: Diffusion behavior of extractives compound classes. (A): Compound class concentration, detected by MS abundance, as a fraction of estimated equilibrium concentration – $C_{\mathrm{MS,rel}}$, as a function of extraction time t. (B): Stacked area plot of time-dependent $C_{\mathrm{MS,rel}}$ and scatter plot (black dots) of cumulative extractives concentration by weight as a fraction of estimated total concentration by weight – $C_{\mathrm{w,rel}}$. The dashed lines indicate the extraction period durations of the extracted boards. (C): Abundance fraction of extractive compound classes removed from boards $C_{\mathrm{MS,rel}}/\sum C_{\mathrm{MS,rel}}$, at the three extraction durations.

## Mechanical Characteristics

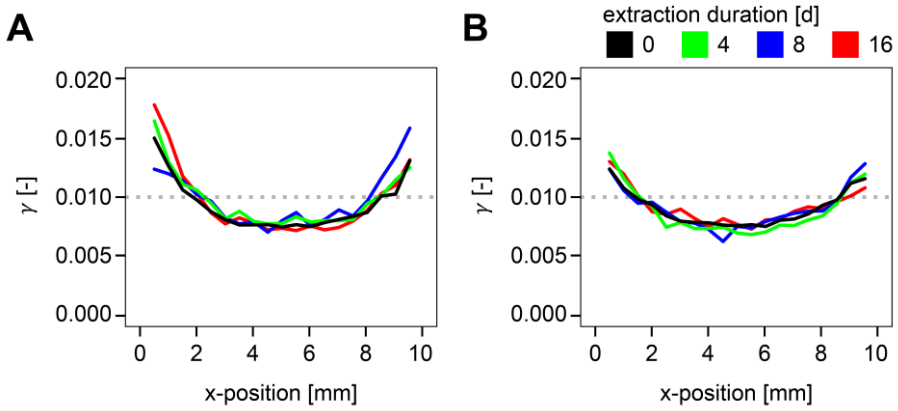


Figure SI–7: Shear strain profiles along the bond line (y=0) at a constant average shear strain ($\overline{\gamma_{bl}}$ = 0.01) in the bond line (dotted grey line) for the tensile shear specimens bonded with MUF (A) and PUR (B). Averaged profiles for specimen groups by extraction duration (see color legend).

For MUF-bonded specimens, the wood failure percentage $WF$, adhesive failure $AF$, and cohesive failure in the bond line $CF$ are plotted over shear strength $\tau_m$ in Figure SI–8A, Figure SI–8C, and Figure SI–8E, respectively. For PUR-bonded specimens, $WF$, $AF$, and $CF$ are plotted over shear strength $\tau_m$ in Figure SI–8B, Figure SI–8D, and Figure SI–8F, respectively.

$WF$ is negatively correlated ($p < 0.0001$) to $\tau_m$ with $R^2 = 0.37$ and 0.09 for MUF-bonded and PUR-bonded specimens, respectively. Correspondingly, $AF$ is positively correlated ($p < 0.0001$) to $\tau_m$ with $R^2 = 0.31$ and 0.09 for MUF-bonded and PUR-bonded specimens, respectively and $CF$ is positively correlated to $\tau_m$ with $R^2 = 0.20$ ($p < 0.0001$) and 0.04 ($p < 0.003$) for MUF-bonded and PUR-bonded specimens, respectively.

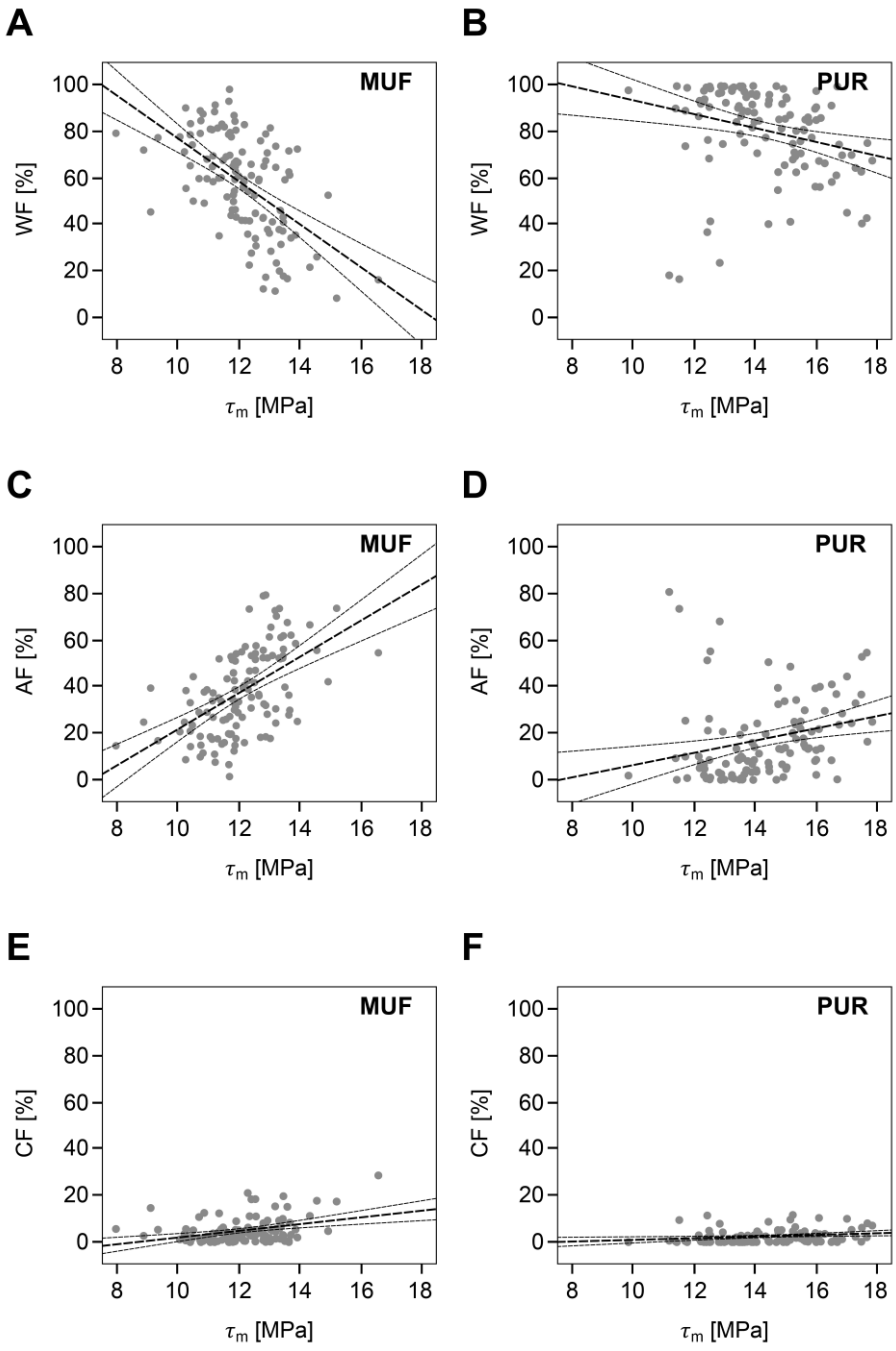


Figure SI–8: Failure modes as a function of the tensile shear specimens' strength $\tau_m$. Area fractions of wood failure (WF – A for MUF, B for PUR), adhesive failure (AF – C for MUF, D for PUR), and cohesive failure in the adhesive (CF – E for MUF, F for PUR). The black dashed lines indicate the linear regression of the individual results and the confidence band ($\alpha = 0.05$).

## Bond Line Morphology

In Figure SI–9A, the areal fraction of cavities in the bond line – the porosity $\phi$ – of specimens bonded with MUF adhesive is shown for varying $ED$. The average porosity was $\bar{\phi}$ = 0.6% for non-extracted wood specimens, and 0.4, 0.3, and 0.3% in the cases of 4, 8 and 16 d extraction duration, respectively.

In Figure SI–9B, the porosity $\phi$ of PUR-bonded specimens for varying $ED$ is shown. The average porosity was $\bar{\phi}$ = 0.5% for non-extracted wood specimens, and 1.4, 2.3, and 1.8% in the cases of 4, 8 and 16 d extraction duration, respectively.

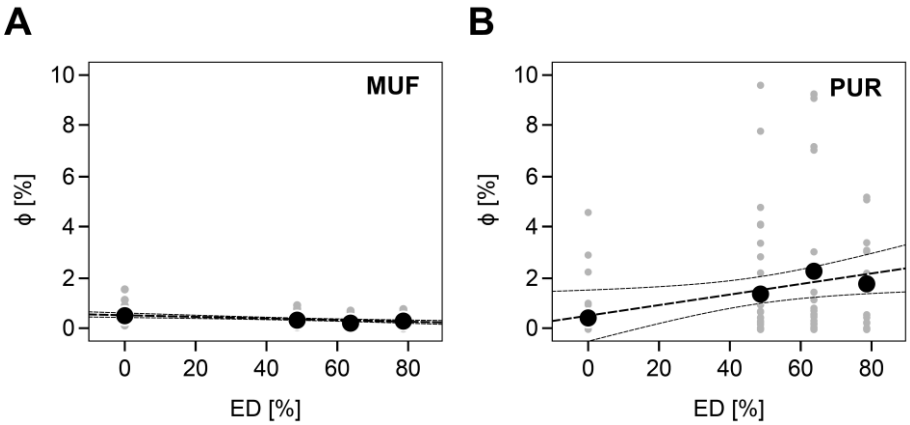


Figure SI–9: Bond line porosity $\phi$ of tensile shear specimens shown as a function of the extraction degree ED for MUF-bonded (A) and PUR-bonded (B) specimens. Small dots indicate individual results, and the large dots indicate the average result per specimen group. The dashed lines indicate the linear regression estimate and the confidence band (α = 0.05).